

22. A simple calculation indicates that the magnitudes of  $V_s^+$  and  $V_s^-$  are on the order of a few tens to hundreds of volts. In practice, if we consider the polarization and dielectric screening in the calculation, the local potential is much smaller than the numbers given by the equations here. An accurate calculation of the potential distribution as a result of the ionic charges introduced by the PZ effect and the surface charges caused by boundaries must be solved numerically and self-consistently. In our analysis, a correct magnitude and sign of the potential is sufficient for illustrating the physical model.
23. S. Hasegawa, S. Nishida, T. Yamashita, H. Asahi, *J. Ceramic Proc. Res.* **6**, 245 (2005).

24. R. F. Pierret, *Semiconductor Device Fundamentals* (Addison-Wesley, Reading, MA, 1996), chapter 14.
25. W. I. Park, G. C. Yi, J. W. Kim, S. M. Park, *Appl. Phys. Lett.* **82**, 4358 (2003).
26. Y. Huang *et al.*, *Science* **294**, 1313 (2001).
27. A. Bachtold, P. Hadley, T. Nakanishi, C. Dekker, *Science* **294**, 1317 (2001); published online 4 October 2001 (10.1126/science.1065824).
28. J. Chen *et al.*, *Science* **310**, 1171 (2005).
29. U.S. patent pending.
30. Supported by NSF grant DMR 9733160, the NASA Vehicle Systems Program and Department of Defense Research and Engineering, and the Defense Advanced Research

Projects Agency. We thank X. Wang, W. L. Hughes, J. Zhou, and J. Liu for their help.

### Supporting Online Material

www.sciencemag.org/cgi/content/full/312/5771/242/DC1

SOM Text

Figs. S1 to S6

Table S1

Movies S1 and S2

19 December 2005; accepted 10 March 2006

10.1126/science.1124005

# Control of Electron Localization in Molecular Dissociation

M. F. Kling,<sup>1</sup> Ch. Siedschlag,<sup>1</sup> A. J. Verhoef,<sup>2</sup> J. I. Khan,<sup>1</sup> M. Schultze,<sup>2</sup> Th. Uphues,<sup>3</sup> Y. Ni,<sup>1</sup> M. Uiberacker,<sup>4</sup> M. Drescher,<sup>3,5</sup> F. Krausz,<sup>2,4</sup> M. J. J. Vrakking<sup>1</sup>

We demonstrated how the subcycle evolution of the electric field of light can be used to control the motion of bound electrons. Results are presented for the dissociative ionization of deuterium molecules ( $D_2 \rightarrow D^+ + D$ ), where asymmetric ejection of the ionic fragment reveals that light-driven intramolecular electronic motion before dissociation localizes the electron on one of the two  $D^+$  ions in a controlled way. The results extend subfemtosecond electron control to molecules and provide evidence of its usefulness in controlling reaction dynamics.

**F**ew-cycle laser light with a controlled evolution of the electric field  $E(t) = a(t) \times \cos(\omega t + \phi)$ , with amplitude  $a(t)$ , frequency  $\omega$ , and carrier envelope phase  $\phi$  ( $I$ ), has recently allowed the steering of the motion of electrons in and around atoms on a subfemtosecond time scale. Manifestations of this control include the reproducible generation and measurement of single subfemtosecond pulses (2, 3) and controlled electron emission from atoms (4, 5). Here we address the question of whether this control can be extended to electron wave packets in molecules and, if so, can light-field-driven electronic motion affect reaction dynamics?

Many of the processes in terms of which strong-field molecular interactions are presently interpreted (such as bond softening and enhanced ionization) were discovered in experimental and theoretical work on  $H_2$  and its isotopes HD and  $D_2$  [see (6) and references therein]. The role of phase control in the dissociation of hydrogen has recently been addressed in a few theoretical studies (7–9). We present experiments on the dissociation of  $D_2^+$  into  $D^+ + D$  by intense few-cycle laser pulses with controlled field evolution and report a pronounced dependence of the direction of the  $D^+$  ejection (and hence of the localization of the electron in the system) on the waveform driving the reaction. Quantum-

classical computations reveal that light-field control of molecular electron dynamics is responsible for the observed phenomenon.

The dynamics of molecules in intense laser fields typically includes ionization and dissociation. The dissociation of  $D_2$  in intense laser fields is known to involve several pathways whose relative importance depends on intensity and pulse duration (6). The formation of fragment ions oc-

curs via a two-step mechanism (Fig. 1A) in which initially the molecule is ionized by the laser field (Fig. 1A, red arrow) and a vibrational wave packet is launched in the  $1s\sigma_g^+$  state. Breakup of the  $D_2^+$  ion is triggered by excitation to a repulsive state or after double ionization.

In the single-ionization pathways, excitation of bound  $D_2^+$  (such as to the  $2p\sigma_u^+$  state in Fig. 1A) by recollision of the first electron [recollision excitation (RCE), green line] or directly by the laser field [sequential excitation (SE), blue line] leads to dissociation and the formation of a  $D^+$  ion and a D atom. For example, in recent molecular clock studies, vibrational motion in  $D_2^+$  was time-resolved by exploiting RCE (10, 11). Additional dissociation mechanisms can be understood by considering that molecular potentials are modified by strong laser fields. Bond softening (BS, purple line) (12) occurs when energy gaps open up at avoided crossings between adiabatic field-dressed potential energy curves.

In double-ionization pathways, the formation of  $D_2^{2+}$  is followed by a second ionization

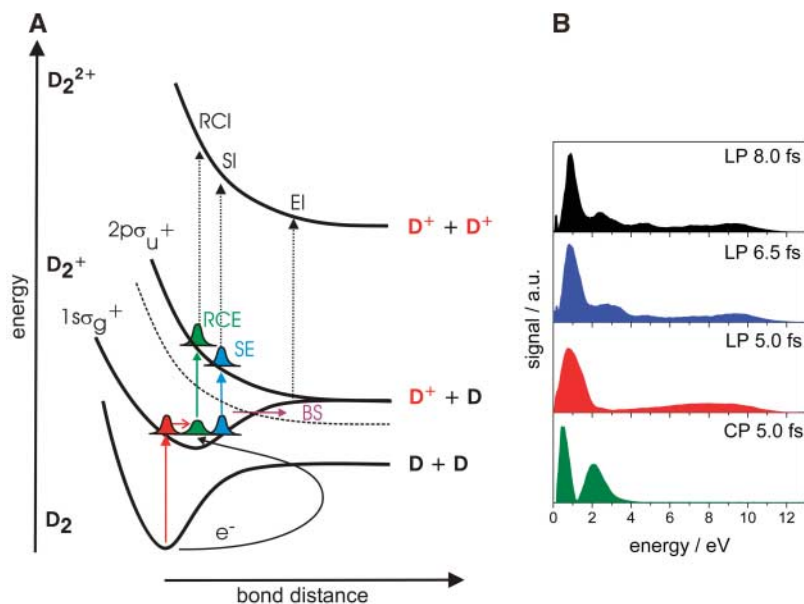


**Fig. 1.** (A) Pathways for the production of  $D^+$  ions from  $D_2$  by dissociation of the molecular ion (through BS, SE, or RCE) or by Coulomb explosion (through RCI, SI, or EI). BS occurs when the avoided crossing between diabatic potentials that are dressed by the laser field gives rise to dissociation from vibrational levels that were originally bound (12). (B)  $D^+$  kinetic energy spectra for dissociation of  $D_2$  by 5- to 8-fs linearly polarized (LP) and 5-fs circularly polarized (CP) laser pulses without phase stabilization, at  $I = 1.2 \pm 0.2 \times 10^{14} \text{ W cm}^{-2}$  and  $I = 2.4 \pm 0.2 \times 10^{14} \text{ W cm}^{-2}$ , respectively.

<sup>1</sup>FOM Instituut voor Atoom en Molecuul Fysica (AMOLF), Kruislaan 407, 1098 SJ Amsterdam, Netherlands. <sup>2</sup>Max-Planck-Institut für Quantenoptik, Hans-Kopfermann-Strasse 1, D-85748 Garching, Germany. <sup>3</sup>Fakultät für Physik, Universität Bielefeld, Universitätsstrasse 25, D-33615 Bielefeld, Germany. <sup>4</sup>Department für Physik, Ludwig-Maximilians-Universität München, Am Coulombwall 1, D-85748 Garching, Germany. <sup>5</sup>Institut für Experimentalphysik, Universität Hamburg, Luruper Chaussee 149, D-22761 Hamburg, Germany.

step via recollision [recollision ionization (RCI)] or via the laser field [sequential ionization (SI)]. Enhanced ionization (EI) takes place when the vibrational wave packet reaches a transition region where electron localization occurs and where (anti)-bonding molecular orbitals turn into atomic orbitals. Double ionization (via RCI, SI, or EI) leads to the breakup of the molecule by Coulomb repulsion between the two  $D^+$  ions. Two momentum-matched  $D^+$  ions are emitted symmetrically along the molecular axis, irrespective of the shape of the driving fields. To address the feasibility of reaction control by means of steering electronic motion, we therefore have to investigate the BS, SE, and RCE pathways and keep double ionization at a minimum.

We have studied the dissociation of  $D_2^+$  in a few-cycle laser field by measuring the emission of  $D^+$  as a probe of the location (or absence) of the electron.  $D^+$  fragment kinetic energy and angular distributions were retrieved using the velocity-map imaging technique (13). For a description of the experimental apparatus, see the supporting online material (SOM). In general, all the pathways illustrated in Fig. 1 contribute to the  $D^+$  kinetic energy spectra. Their relative importance sensitively depends on the intensity and duration of the laser (6). Figure 1B shows  $D^+$  kinetic energy spectra recorded for linearly and circularly polarized laser pulses with durations of 5 to 8 fs at peak intensities ( $I$ ) of  $I = 1.2 \pm 0.2 \times 10^{14} \text{ W cm}^{-2}$  and  $I = 2.4 \pm 0.2 \times 10^{14} \text{ W cm}^{-2}$ , respectively.

Previous studies (14–16) suggest that  $D^+$  ions with energies below 3 eV originate from BS (at  $\sim 0.9$  eV) and EI (at  $\sim 2.5$  eV). Above 3 eV, contributions may arise from SE/SI and RCE/RCI. In our experiment, the disappearance of the  $D^+$  signal above 3 eV upon changing the polarization from linear to circular (while maintaining the peak electric field of the laser) indicates that recollision is responsible for the

creation of the high-energy fragments (Fig. 1B). Decreasing the pulse duration from 8 to 5 fs suppresses spectral components assigned to double ionization. Light-field control of molecular dissociation was therefore pursued with phase-stabilized 5-fs laser pulses.

Figure 2 shows a cut through the  $D^+$  three-dimensional momentum distribution in Cartesian coordinates ( $p_x, p_y$ ) at  $p_z = 0$ , for a 5-fs,  $1 \times 10^{14} \text{ W cm}^{-2}$  laser field without phase stabilization. The laser propagated along the  $x$  axis ( $\theta = 90^\circ/270^\circ$ ) and was polarized along the  $y$  axis ( $\theta = 0^\circ/180^\circ$ ). In agreement with previous studies (17), the BS (0 to 2 eV) and the weak EI channel (2 to 3 eV) that appear in the center of the image show relatively narrow angular distributions. A nearly isotropic distribution is measured for higher energies (3 to 10 eV) and is a typical signature of recollision-induced fragmentation (15). No difference in the up versus down emission of  $D^+$  ions (along the laser polarization axis) is observed without phase stabilization.

In an attempt to control and probe the final location of the electron in the  $D_2^+$  dissociation,  $D^+$  images were recorded while changing the carrier envelope phase  $\phi$ . The angle-integrated asymmetry in the  $D^+$  emission was evaluated as a function of energy  $W = p^2/2m$  and  $\phi$  via

$$A(W, \phi) = \frac{P_{up}(W, \phi) - P_{down}(W, \phi)}{P_{up}(W, \phi) + P_{down}(W, \phi)}$$

with

$$P_{up}(W, \phi) = \int_{330}^{360} d\theta \int_0^{360} d\phi P(W, \theta, \phi, \phi) \sin \theta + \int_0^{30} d\theta \int_0^{360} d\phi P(W, \theta, \phi, \phi) \sin \theta$$

and

$$P_{down}(W, \phi) = \int_{150}^{210} d\theta \int_0^{360} d\phi P(W, \theta, \phi, \phi) \sin \theta$$

with  $\theta$  and  $\phi$  being the polar and azimuthal angles, respectively.

We chose to analyze the ion emission within a restricted angular range because (as will become clear) our ability to control electron motion in  $D_2^+$  requires that the laser couple the two lowest-lying electronic states. For molecules aligned orthogonally to the laser polarization axis, this coupling is absent.

Figure 3A depicts the angle-integrated  $D^+$  energy spectrum obtained with 5-fs laser pulses with a peak intensity of  $I = 1 \times 10^{14} \text{ W cm}^{-2}$  and a randomly varying carrier envelope phase. Figure 3B reveals how phase locking results in a nonzero asymmetry  $A(W, \phi)$  as a function of the kinetic energy  $W$  of the  $D^+$  fragments ( $y$  axis) and the laser phase  $\phi$  ( $x$  axis). Regions where the asymmetry oscillates as a function of the phase represent conditions where the direction of the  $D^+$  emission, and hence the localization of the electron in the dissociation process, is effectively controlled by the subcycle evolution of the laser field driving the dissociation. The extent of the control is further illustrated in Fig. 3C, which displays a series of curves where  $A(W, \phi)$  is integrated over selected energy intervals. The highest degree of asymmetry with a modulation depth of  $\sim 50\%$  is observed between 3 and 8 eV. A very small phase dependence is seen between 0 and 3 eV. Asymmetric  $D^+$  ejection is observed predominantly at kinetic energies that are virtually absent in a circularly polarized field, suggesting that electron-ion recollision is a vital element in the mechanism responsible for the observed phase control.

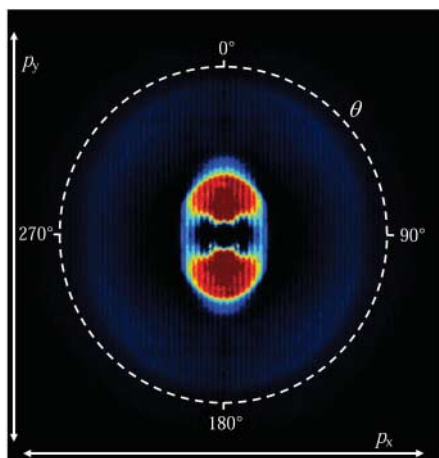


**Fig. 2.** Two-dimensional  $D^+$  momentum image for  $D_2$  dissociation in a 5-fs,  $1 \times 10^{14} \text{ W cm}^{-2}$  laser field without phase stabilization.

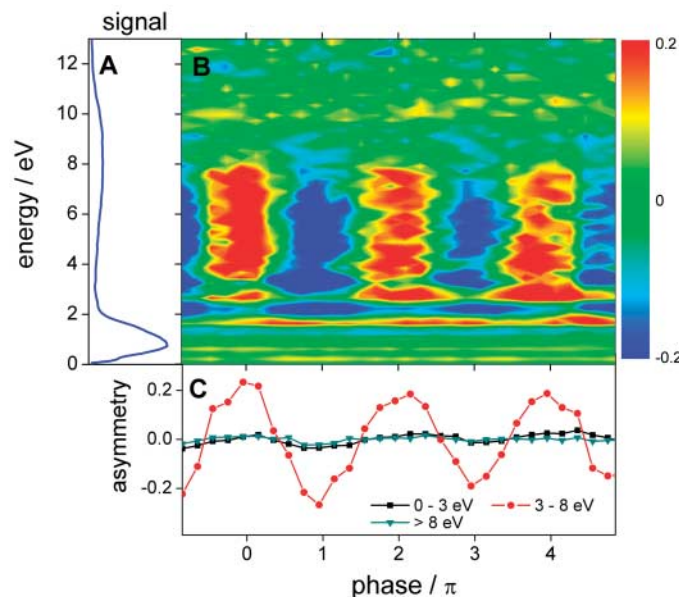


**Fig. 3.** (A)  $D^+$  kinetic energy spectrum for  $D_2$  dissociation with 5-fs,  $1 \times 10^{14} \text{ W cm}^{-2}$  laser pulses without phase stabilization. (B) Map of asymmetry parameter  $A(W, \phi)$  as a function of the  $D^+$  kinetic energy and carrier envelope phase  $\phi$  (measured over a range of  $6\pi$  with a step size of  $\Delta\phi = 0.1\pi$ ). (C) Integrated asymmetry over several energy ranges versus carrier envelope phase  $\phi$ .

To gain qualitative insight into the mechanism responsible for the observed phase-controlled asymmetry in the dissociation of  $D_2^+$ , we modeled the laser-driven motion of the two nuclei and the bound electron by numerically solving the time-dependent Schrödinger equation (see the SOM for details). As in previous studies (18), the process is modeled in terms of the  $1s\sigma_g^+$  and  $2p\sigma_u^+$  electronic states, and the molecule is assumed to be aligned along the laser polarization axis.

In our modeling, the  $D_2^+$  molecular ion is formed in a single ionization event that occurs at the maximum of the laser electric field. This ionization produces a vibrational wave packet in the  $1s\sigma_g^+$  ground electronic state that mimics the ( $v=0$ ) vibrational wave function of the  $D_2$  ground state. Population transfer from the  $1s\sigma_g^+$  ground electronic state to the  $2p\sigma_u^+$  excited electronic state is introduced at a delay of 1.7 fs after ionization [corresponding to the first recollision time (10)]. Later recollision events are efficiently suppressed with short laser pulses (15). Because of the strongly repulsive nature of the  $2p\sigma_u^+$  state, the excited  $D_2^+$  molecule dissociates and the momentum-matched D and  $D^+$  fragments acquire a large kinetic energy ( $E_k$  up to 10 eV). During the dissociation, the laser field transfers part of the  $2p\sigma_u^+$  population to the  $1s\sigma_g^+$  state, producing a dissociative wave packet with a large excess kinetic energy. The emerging coherent superposition of the two electronic states results in a time-dependent localization of the electron density on the upper or lower nucleus due to the gerade and ungerade nature of the two states (7, 9, 19).

In Fig. 4, the temporal evolution of the laser field and the occupations of the  $1s\sigma_g^+$  and  $2p\sigma_u^+$  electronic states are depicted in (A) and

(B), respectively. A time-dependent electron localization parameter quantifying the localization on the upper/lower nucleus (for definition, see the SOM) is displayed in (C). By the time the molecule has dissociated (with the internuclear distance reaching  $\sim 15$  atomic units), the electron density is found to localize predominantly on the lower D atom. A simple shift of the carrier envelope phase  $\phi$  by  $\pi$  reverses the field and turns the direction of emission of the ionic/atomic fragment opposite, in agreement with our experimental observation. To the best of our knowledge, this is the first demonstration of direct light-field control of a chemical reaction via the steering of electronic motion.

Let us consider the electron localization dynamics after the recollision in more detail. Initially, the  $1s\sigma_g^+$  state is hardly populated by the laser-induced coupling, and the energy gap  $\Delta W(t) = \hbar\omega(t)$  between the binding  $1s\sigma_g^+$  and repulsive  $2p\sigma_u^+$  states is much larger than the laser photon energy. Hence, the electronic wave function can respond nearly instantaneously to changes in the laser field, and the electron localization parameter (Fig. 4C) oscillates with a small amplitude at the frequency of the light pulse. As the eigenfrequency  $\omega(t)$  of the two-level system decreases because of the increasing bond length, the laser field starts populating the lower state substantially, strongly increasing the extent of electron localization. In our calculations, the electron wave packet keeps evolving with the instantaneous eigenfrequency  $\omega(t)$  as the laser field strength approaches zero (for  $t > 7$  fs). The oscillation of the electron localization ceases when the interatomic barrier that builds up between the two  $D^+$  ions can no longer be overcome by the electron. In the experiment, because of a

nonzero background of the few-cycle pulses ( $<10\%$  in intensity), a laser field may still be present when the molecule breaks up and contribute to the asymmetry (20).

The field-controlled electron dynamics demonstrated in this work does not rely on electron recollision. In fact, control of electron dynamics in molecules can also be achieved by preparing a coherent electronic superposition state by photoexcitation (7, 19, 21, 22). In contrast with the current experiment, the photoexcitation will permit the creation of an electron wave packet at the beginning of the reaction, thereby offering a greater flexibility for its subsequent light-field control. This approach will also be applicable in neutral molecules.

## References and Notes

1. A. Baltuška *et al.*, *Nature* **421**, 611 (2003).
2. R. Kienberger *et al.*, *Nature* **427**, 817 (2004).
3. E. Goulielmakis *et al.*, *Science* **305**, 1267 (2004).
4. G. G. Paulus *et al.*, *Phys. Rev. Lett.* **91**, 253004 (2003).
5. F. Lindner *et al.*, *Phys. Rev. Lett.* **95**, 040401 (2005).
6. J. H. Posthumus, *Rep. Prog. Phys.* **67**, 623 (2004).
7. A. D. Bandrauk, S. Chelkowski, H. S. Nguyen, *Int. J. Quant. Chem.* **100**, 834 (2004).
8. V. Roudnev, B. D. Esry, I. Ben-Itzhak, *Phys. Rev. Lett.* **93**, 163601 (2004).
9. H. Niikura, D. M. Villeneuve, P. B. Corkum, *Phys. Rev. A* **73**, 021402 (2006).
10. H. Niikura *et al.*, *Nature* **417**, 917 (2002).
11. H. Niikura *et al.*, *Nature* **421**, 826 (2003).
12. P. H. Bucksbaum, A. Zavrinyev, H. G. Muller, D. W. Schumacher, *Phys. Rev. Lett.* **64**, 1883 (1990).
13. A. T. J. B. Eppink, D. H. Parker, *Rev. Sci. Instr.* **68**, 3477 (1997).
14. A. S. Alnaser *et al.*, *Phys. Rev. Lett.* **91**, 163002 (2003).
15. A. S. Alnaser *et al.*, *Phys. Rev. Lett.* **93**, 183202 (2004).
16. H. Sakai *et al.*, *Phys. Rev. A* **67**, 063404 (2003).
17. K. Sändig, H. Figger, T. W. Hänsch, *Phys. Rev. Lett.* **85**, 4876 (2000).
18. I. Kawata, H. Kono, Y. Fujimura, *J. Chem. Phys.* **110**, 11152 (1999).
19. G. L. Yudin, S. Chelkowski, J. Itatani, A. D. Bandrauk, P. B. Corkum, *Phys. Rev. A* **72**, 051401 (2005).
20. M. Y. Ivanov, P. B. Corkum, P. Dietrich, *Laser Phys.* **3**, 375 (1993).
21. H. Niikura, D. M. Villeneuve, P. B. Corkum, *Phys. Rev. Lett.* **94**, 083003 (2005).
22. P. Krause, T. Klamroth, P. Saalfrank, *J. Chem. Phys.* **123**, 074105 (2005).
23. We thank J. Rauschenberger for experimental support and acknowledge valuable discussions with B. Esry, P. Corkum, and H. Niikura. We are grateful for financial support from the Marie Curie Research Training Network XTRA (grant no. MRTN-CT-2003-505138) and a Marie Curie Intra-European Fellowship (no. MEIF-CT-2003-500947) (M.F.K.). The research of M.F.K., Ch.S., J.I.K., Y.N., and M.J.J.V. is part of the research program of the Stichting voor Fundamenteel Onderzoek der Materie (FOM), which is financially supported by the Nederlandse Organisatie voor Wetenschappelijk Onderzoek (NWO).

## Supporting Online Material

www.sciencemag.org/cgi/content/full/312/5771/246/DC1

SOM Text

Figs. S1 and S2

References

15 February 2006; accepted 15 March 2006  
10.1126/science.1126259

**Fig. 4.** (A) Electric field of the 5-fs,  $1 \cdot 10^{14}$  W  $\text{cm}^{-2}$  pulse used in the calculations, with carrier envelope phase  $\phi = 0$ . (B) Time-dependent populations of the  $1s\sigma_g^+$  and  $2p\sigma_u^+$  states of  $D_2^+$  after excitation through recollision. (C) Temporal evolution of the electron localization parameter starting from the time of recollision. (D) Time dependence of the eigenfrequency  $\omega(t)$  of the two-level system versus the laser frequency  $\omega_0$  (frequencies are given in atomic units). The vertical dashed purple line marks the time of recollision in all panels.

